Transfer Impedance at High Frequencies

H.G. Krauthäuser, J. Nitsch S. Tkachenko, N. Korovkin, and H.-J. Scheibe
Otto-von-Guericke-University, Universitaetsplatz 2, D-39106 Magdeburg, Germany Email: hgk@ieee.org

***Abstract*— A partially new analysis method to determine the transfer impedance (TI) of coaxial cables is proposed. The method involves two steps. The first (experimental) step consists in the determination of the voltage between the interior wire and the cable shield which is exposed to an exterior TEM field. In the experiment the investigated cable forms a semicircular loop, whose plane is orthogonal to an ideally conductive plane. The measurements have been performed in a GTEM cell. In the second step the calculation of the TI of the cable is carried out. These calculations are based on the analytical solutions for the current in the cable shield.**

It is shown that with the proposed method — in principal — one can determine the complex transfer impedance for frequencies up to 10 GHz for typical cable diameters. Furthermore, the experimental setup is rather simple compared to other methods.

At the moment, the evaluation of the experimental data is limited to 600–700 MHz, approximately. This is due to the lack of a more adequate Green's function for the description of the loop in the field inside the GTEM cell.

I. Introduction

The urgency to determine the cable TI at high frequencies is well known. Theoretical and experimental results are found in [1]–[4]. An exhaustive review of up to date theoretical and experimental results is presented in [5]. The problem of determining $Z_t(j\omega)$ is very pressing at present [6]–[10]. It is shown in our papers [11], [12] that the difficulties to experimentally determine the cable TI considerably grow with increasing frequency. Operational frequencies of cables and noise frequencies constantly grow. Therefore, the development of new and the perfection of existing designs of cable shields is necessary. There is a significant interest for designing noise-resistant electronic devices and signal transmission systems.

In this work we will examine an experimental setup for the TI determination with the aid of a loop-method [13]. In Section III, we will consider a new method to calculate the current of the tested cable shield. This current is needed in the loop-method for the TI calculation from the experimental data. The final part of this paper (Section IV) presents the results of the experiment.

II. Experimental setup of the Loop-Method

Recently, measurements of the TI at microwave frequencies have been described by Sali using a quite sophisticated experimental setup [14].

The simple experimental installation of the loop-method to determine the TI is presented in Fig. 1. The tested cable forms a semi-circular loop above an ideally conducting plane. The current I in the cable shield is induced by an external plane electromagnetic wave (this differ from the original setup described in [13]). The voltage U_1, induced between the interior wire and the shield of the cable is measured. Measurements can preferably be carried out in an anechoic chamber or in a GTEM cell.

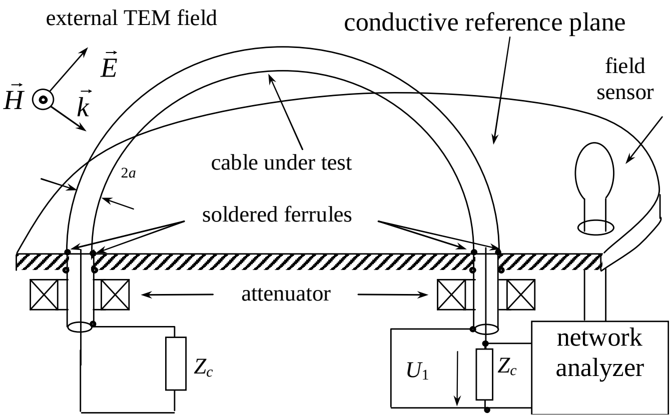

Fig. 1. The scheme of the experimental setup of the loop-method.

The current I flowing along the cable shield and inducing the voltage U_1 through the TI mechanism does not flow along plugs connecting the tested cable with loads or the measuring equipment. This eliminates one essential source of an experimental error. According to estimates in [15], [16] the TI increases through cable joints up to 13dB/Dec. This is confirmed also by our measurements [11], [12].

The geometry of the experimental setup is rather simple and allows to calculate the current under the assumptions that the current density is uniformly distributed over the cross-section perimeter of the cable shield, and the wavelength λ of the exciting field satisfies the inequality $\lambda > 8a$, where a is the shield radius [17]. The latter inequality yields a frequency $f < 10$ GHz for $a = 4$ mm, which gives an upper frequency bound for the application of the loop-method for cables with such radii. Therefore, the loop-method is a potential method to be used to measure the TI at high frequencies. As will be shown in Section III, the functions used in calculating the TI have no sharp peaks. This allows us to obtain stable results with reasonable measurement errors. Moreover, with the increase in frequency, these functions become smoother, which in many respects is caused by radiation losses.

III. Calculation of the Transfer Impedance Applying the Loop-Method

In this section, we consider theoretical aspects of the TI calculation. At the beginning, we examine the so-called "external problem" consisting of the determination of the cable shield

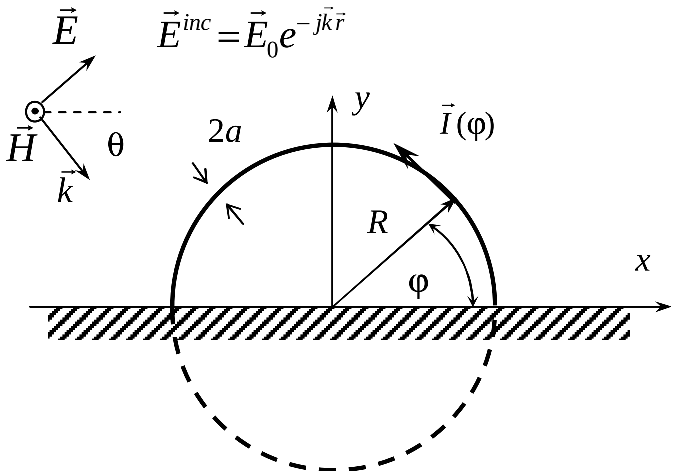

Fig. 2. The external problem.

current, and later on the "internal problem", the problem to determine the cable TI from a voltage measurement.

A. The External Problem

Let us consider a semi-circular loop near a perfectly conducting ground (see Fig. 2). The loop is excited by a plane wave. The current $I(l)$ and the potential $\Phi(l)$ (in the Lorenz gauge), induced in the loop are described by the following system of integro-differential equations [17], [18] (in the thin-wire approximation):

$$\frac{\partial\Phi(l)}{\partial l} + j\omega\frac{\mu_0}{4\pi}\int_0^{\pi R} g_A(k,l',l,R,a)I(l')dl' = E_l^0(l) \quad (1)$$

$$\int_0^{\pi R} g_\Phi(k,l',l,R,a)\frac{\partial I(l')}{\partial l'}dl' + j\omega 4\pi\varepsilon_0\Phi(l) = 0 \quad (2)$$

where

$$\begin{aligned} g_\Phi(k,l',l,R,a) =& g(k,l'-l,R,a) \\ &- g(k,l'+l,R,a) \\ g_A(k,l',l,R,a) =& \cos\left(\frac{l'-l}{R}\right) g(k,l'-l,R,a) \\ &+ \cos\left(\frac{l'+l}{R}\right) g(k,l'+l,R,a) \\ g(k,l,R,a) =& \frac{e^{-jk\sqrt{4R^2\sin^2(l/2R)+a^2}}}{\sqrt{4R^2\sin^2(l/2R)+a^2}} \end{aligned} \quad (3)$$

l ($0 \le l \le \pi R$) is the length along the semi-circle.

Because all physical quantities are periodical along the circle, we are looking for the solution as Fourier series. For the exciting tangential electric field, we have:

$$\begin{aligned} E_l^0(l) = \sum_{m=0}^{\infty} E_{m,l}^0\sqrt{\varepsilon_{0m}/\pi}\cos(m\varphi) = \sum_{m=0}^{\infty} E_{m,l}^0(l) \\ \varepsilon_{0m} = \quad 2 - \delta_{m,0}, \quad \varphi = l/R \end{aligned} \quad (4)$$

In the case of the excitation by a plane wave (also taking into account the reflection from the ground) one finds

$$\begin{aligned} E_{m,l}^0 =& E_0\sqrt{\varepsilon_{0m}\pi}(-j)^{m+1}\cdot \\ & (J_{m+1}(kR) - J_{m-1}(kR))\cos(m\theta) \end{aligned} \quad (5)$$

where $J_m(x)$ is the Bessel function of order m, and θ is the angle of incidence. For the induced current $I(l)$ we obtain the following classical result [19]–[21]:

$$I(l) = \sum_{m=0}^{\infty} I_m\sqrt{\frac{\varepsilon_{0m}}{\pi}}\cos(m\varphi) \quad (6)$$

$$I_m = -\frac{4\pi jkE_{m,l}^0}{\eta_0 R}\cdot\frac{1}{\frac{k^2}{2}(g_{m+1}-g_{m-1}) - k_m^2 g_m} \quad (7)$$

with the modal wave number $k_m = m/R$ and

$$\begin{aligned} g_m(k,R,a) =& \int_0^{2\pi}\frac{e^{jm\varphi - jk\sqrt{4R^2\sin^2(\varphi/2)+a^2}}}{\sqrt{4R^2\sin^2(\varphi/2)+a^2}}d\varphi \\ =& 2\pi\int_0^{\infty}\frac{e^{-a\sqrt{k_\rho^2-k^2}}}{\sqrt{k_\rho^2-k^2}}k_\rho J_m^2(k_\rho R)dk_\rho \end{aligned} \quad (8)$$

For the thin wire $a \ll 1/k, R$, it is possible to write the function $g_m(k,R,a)$ as [19], [22]:

$$\begin{aligned} g_m(k,R,a) \simeq& \frac{2}{R}\cdot(\ln(2R/a) - \gamma - \psi(1/2 - |m|)) \\ &+ \frac{\pi}{R}\int_0^{2kR}\left(E_{2|m|}(x) - jJ_{2|m|}(x)\right)dx \end{aligned} \quad (9)$$

where $E_{2|m|}(x)$ is the Weber-Function, $\psi(x)$ is the logarithmic derivative of the Gamma-function.

The results for the current distribution along the circle agree well with these obtained by numerical methods (MoM, NEC).

B. The Internal Problem

For the definition of the induced currents and voltages in the internal circuit (see Fig. 1) (the so-called internal problem) we have the following system of Telegraphers equations (the $\tilde{}$ refers to internal quantities) [5]:

$$\begin{aligned} \frac{d\tilde{U}(l)}{dl} + j\omega\tilde{L}'\tilde{I}(l) = \tilde{E}_z^e(l) \\ \frac{d\tilde{I}(l)}{dl} + j\omega\tilde{C}'\tilde{U}(l) = 0 \end{aligned} \quad (10)$$

with the boundary conditions

$$\tilde{U}(0) = -\tilde{Z}_1\cdot\tilde{I}(0) \qquad \tilde{U}(L) = \tilde{Z}_2\cdot\tilde{I}(L) \quad (11)$$

In Eq. (10) $\tilde{L}'$ and $\tilde{C}'$ are the per-unit length internal inductance and capacitance, respectively:

$$\tilde{L}' = \frac{\mu_0}{2\pi}\ln\left(\frac{a}{\tilde{a}}\right), \qquad \tilde{C}' = \frac{2\pi\varepsilon\varepsilon_0}{\ln\left(\frac{a}{\tilde{a}}\right)} \quad (12)$$

where ε is a relative electric permittivity of the insulating dielectric, and $\tilde{a}$ is the radius of the inner conductor. The

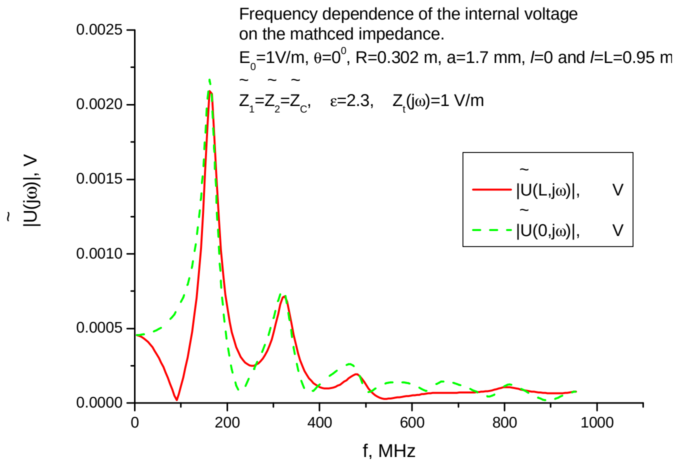

Fig. 3. Frequency dependence of the voltage across the matched impedance.

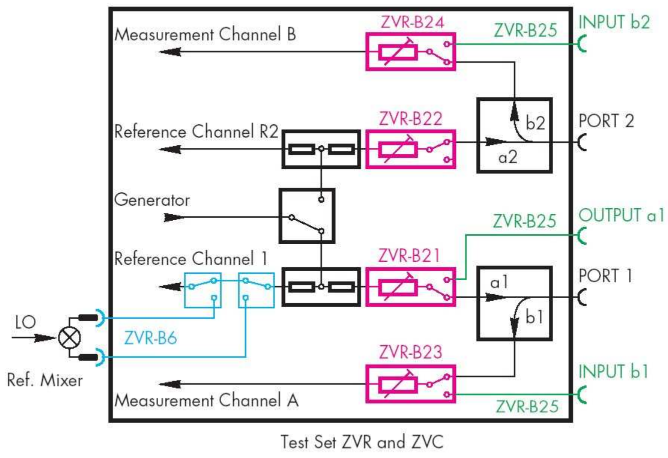

Fig. 4. Internal confi guration of the network analyzer Rohde&Schwarz ZVC (taken from the data sheet).

distributed voltage source $\tilde{E}_z^e(l)$ is defined as $\tilde{E}_z^e(l) = I(l) \cdot Z_t(j\omega)$. Here $I(l)$ is the shield current (solution of the external problem (6)), and $Z_t(j\omega)$ is the TI [5], [23]. We assume here that $Z_t(j\omega)$ is a constant along the line.

For the external current in the form of a forward running wave $I^0 \exp(-jk_m l))$ and with matched loads $\tilde{Z}_1 = \tilde{Z}_2 = \tilde{Z}_c$ it is easy to obtain a solution of (10) and (11) for the load voltages (see also [23], Chapter 5)

$$\tilde{U}_m(0) = I^0 Z_t \frac{j}{2\left(\tilde{k} + k_m\right)} \cdot \left(1 - e^{-j(\tilde{k}+k_m)L}\right) \quad (13)$$

$$\tilde{U}_m(L) = I^0 Z_t \frac{1}{2j\left(\tilde{k} - k_m\right)} \cdot \left(e^{-jk_m L} - e^{-j\tilde{k}L}\right) \quad (14)$$

where $\tilde{k} = k\sqrt{\varepsilon}$ is the wave number of the internal problem, $L = \pi R$ is the length of the system. In (6), for the shield current, we have the forward and backward running waves with the same amplitudes for each mode and, due to linearity of the problem, we can write after some calculations:

$$\tilde{U}(0) = \sum_{m=0}^{\infty} \tilde{U}_m(0), \quad \tilde{U}(L) = \sum_{m=0}^{\infty} \tilde{U}_m(L) \quad (15)$$

with

$$\begin{aligned} \tilde{U}_m(0) = & I_m \sqrt{\frac{\varepsilon_{0,m}}{\pi}} \cdot Z_t(j\omega) \cdot \\ & \frac{\tilde{k}\cos(k_m L) + jk_m \sin(k_m L) - \tilde{k}e^{j\tilde{k}L}}{2j\left(\tilde{k}^2 - k_m^2\right)} \\ \tilde{U}_m(L) = & I_m \sqrt{\frac{\varepsilon_{0,m}}{\pi}} \cdot Z_t(j\omega) \cdot \\ & \frac{\tilde{k}\cos(k_m L) - jk_m \sin(k_m L) - \tilde{k}e^{-j\tilde{k}L}}{2j\left(\tilde{k}^2 - k_m^2\right)} \end{aligned} \quad (16)$$

Here the modal amplitudes of the external current I_m are defined by (7). The frequency dependencies of the functions (15) for the unit TI $Z_t(j\omega)$ and an incident field of unit amplitude are presented in Fig. 3. Then we obtain the TI as the ratio of the values:

$$Z_t(j\omega) = \frac{\tilde{U}_{\text{exp.}}(L, j\omega)}{\tilde{U}_{\text{theor.}}(L, j\omega)\Big|_{Z_t = 1\Omega/\text{m}}} \cdot 1\Omega/\text{m} \quad (17)$$

where $\tilde{U}_{\text{exp.}}(L, j\omega)$ is the experimental internal voltage (across the matched load at the point $l = L$), and $\tilde{U}_{\text{theor.}}(L, j\omega)\Big|_{Z_t = 1\Omega/\text{m}}$ is the theoretical value of function (16) for the unit TI and the electric field which was used in the experiment.

IV. Experimental TI Determination with the Aid of the Loop-Method

Experiments to determine the TI with the aid of the loop-method were conducted in the GTEM cell.

A Rohde&Schwarz ZVC network analyzer was used in a setup for "external measurements", i.e. the internal S-parameter test set was not used. An overview of the interior of the analyzer is given in Fig. 4. For external measurements the switches B21–B24 are in the opposite position. Output a1 is used to drive the amplifiers, inputs b1 and b2 are used to pick up the internal voltage $\tilde{U}_{\text{exp.}}$ and the voltage of the E-field sensor (short rod antenna), respectively. The setup of the loop and the sensor is shown in the photos of Fig. 5.

The advantage of the external measurement setup is that both, the internal voltage and the sensor voltage, can be measured simultaneously. Therefore, instabilities of the amplifier's gain (magnitude and phase variations) are irrelevant.

The primary result of the experiments is ratio $m(f)$ of the two voltages

$$m(f) = \frac{U_{\text{internal}}}{U_{\text{sensor}}} \quad (18)$$

The relationship between the sensor voltage and the E-field is expressed by the antenna factor $\text{AF}_E = E/U_{\text{sensor}}$, which

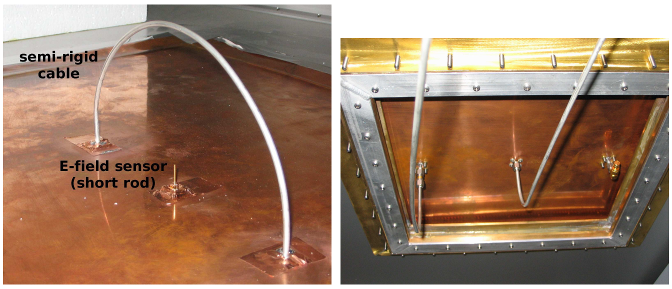

Fig. 5. Measurement setup inside the GTEM cell and connections at the bottom.

is well known from the literature for short rod antennas of height h and radius a ($ka \ll kh \ll 1$) [24]:

$$\mathrm{AF}_E = \frac{Z_0 + Z_L}{Z_L} \cdot \frac{1}{h_e(\vartheta)\cos\psi} \tag{19}$$

Here, Z_L is the load impedance ($50\,\Omega$), Z_0 the antenna input impedance, h_e the effective length of the antenna, ϑ the angle of incidence (here: $\vartheta = \pi/2$), and ψ the polarization mismatch (here: $\psi = 0$). For thin rods Z_0 is approximated by

$$Z_0(f) \simeq -j\frac{\eta_0 \Psi_{\mathrm{dR}}}{2\pi kh}, \quad \Psi_{\mathrm{dR}} = 2\ln\left(\frac{h}{a}\right) - 2 \tag{20}$$

The equivalent height is given by

$$\begin{aligned} h_e(\vartheta) =& \frac{h\Psi_{\mathrm{dR}}}{2(\Omega-3)}\left[\frac{1+k^2h^2G}{1+k^2h^2S/3}\right]\cdot\sin\vartheta \\ G =& \frac{1}{\Omega-3}\left(2\ln\left(\frac{h}{a}\right) - \frac{11}{12}\right) \\ S =& 1 + \frac{3\ln 2 - 1}{\Omega - 3} \\ \Omega =& 2\ln\left(\frac{2h}{a}\right) \end{aligned} \tag{21}$$

Using the antenna factor, we can calculate the internal voltage normalized to unit field strength:

$$\frac{U_{\mathrm{internal}}(f)}{E} = \frac{m(f)}{\mathrm{AF}_E(f)} \tag{22}$$

We performed measurements on two types of shielded cables. One is a type RG58 braided shield cable, and the other one is a semi rigid cable of type EZ-250-TP-M17 (from Huber&Suhner).

A. Results for the RG58 Cable

The experimentally obtained normalized internal voltage for a typ RG58 cable is shown in Fig. 6.

Along with the experimental data, two calculated curves are shown in Fig. 6. These are the magnitude and phase of the internal voltage calculated using the standard formula for the transfer impedance and two different expressions for the m-representation of the Green's functions g_m. The first is the usual free-space formula. The second is a modified version that takes into account that in the GTEM radiation is restricted to one direction. This leads to a first guess for g_m^{GTEM}:

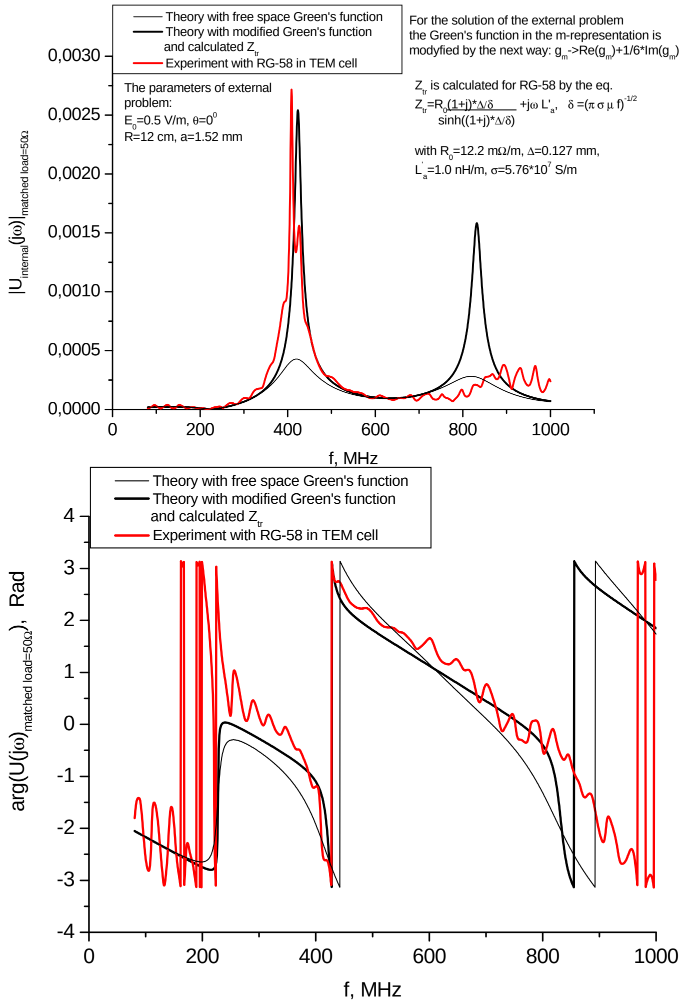

Fig. 6. Magnitude (upper graph) and phase (lower graph) of the normalized internal voltage.

$$g_m \to g_m^{\mathrm{GTEM}} = \Re(g_m) + 1/6 \cdot \Im(g_m) \tag{23}$$

As one can see, the modified version gives better results for the representation of the first resonance, but is less accurate at higher frequencies. A better formula for the Green's function of the given problem would be helpful and is under current investigation.

Since the transfer impedance is calculated from the experimental internal voltages using the analytical solution of the external problem, i.e. using an calculated current on the screen, it is helpful to compare this current with a measurement (using a current probe F2000 from FCC). The results are given in Fig. 7.

Again, we obtain a better agreement using the modified Green's function for the first resonance. Above approximately 700 MHz deviations are visible. Because of the disagreement of the experimental und the theoretical current above 700 MHz the transfer impedance results beyond that limit are less confidential. However, experimental data have been obtained up to 4.2 GHz, and the evaluation will be extended to that

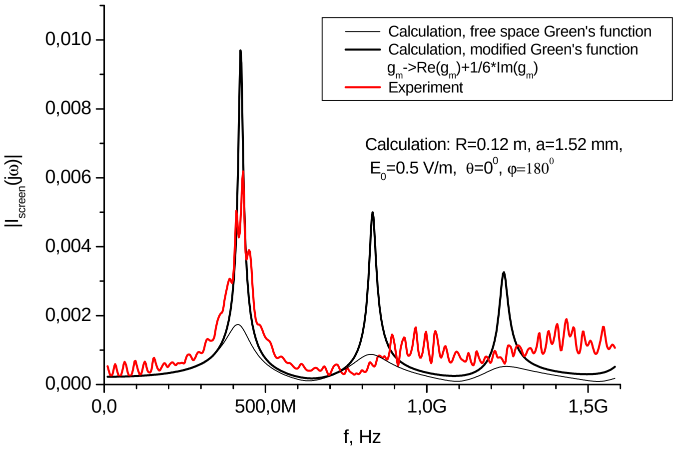

Fig. 7. Magnitude of screen current for E=1 V/m.

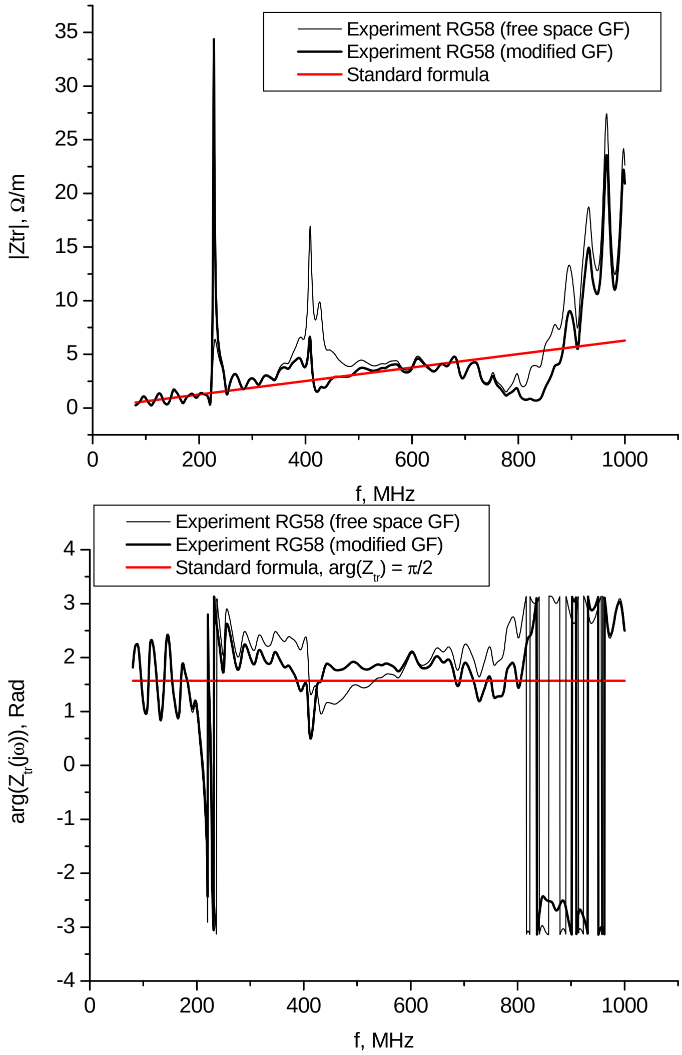

Fig. 8. Magnitude (upper graph) and phase (lower graph) of the transfer impedance of the RG58 cable.

frequency as soon as a more adequate Green's function for the external problem is available.

Using eq. (17), the transfer impedance can be calculated from the experimental data. The results are shown in Fig. 8.

The formula for the theoretical curve in Fig. 8 (standard formula) is Vance formula

$$Z_t = Z_d + j\omega L_a' \tag{24}$$

with empirical data for the parameters of the RG58 cable taken from [5]. Up to 600 MHz a good agreement of both, magnitude and phase, is obtained.

B. Results for the Semi Rigid Cable

Due to the essential better shielding (lower $|Z_t|$), the internal voltages for the semi rigid cable are much smaller compared to these of the RG58 braided shield cable. The measured normalized internal voltages for the semi rigid cable are shown in Fig. 9. Obviously, the overall shapes of the curves for the experiments follow the theoretical data. However, both magnitude and phase do not give the correct absolute values. Especially for the phase there is an offset of nearly 180 degrees for small frequencies. This indicates a possible sign error, e.g. in the data evaluation. This problem is currently investigated.

The transfer impedance calculated from the internal voltage is shown in Fig. 10. Again, discrepancies, both for magnitude and phase, appear in the graphs. As one can see $|Z_t|$ can be calculated from the measurements down to $1 \cdot 10^{-4}$ Ω/m, showing the sensitivity of the method.

V. Conclusion

It has been shown that the loop-method is an experimental simple method for the measurement of the transfer impedance. The method is applicable for frequencies up to 10 GHz (for a cable radius of $\sim$4 mm). That considerably exceeds the possibilities of other methods. However, the use of the method is currently restricted to frequencies up to 700 MHz due to limitations of the Green's function used to solve the external problem. Of course, the transfer admittance has to be addressed too at higher frequencies.

Acknowledgment

The authors would like to thank Dr. D.Giri for helpful discussions.

References

[1] H. Kaden, *Wirbelströme und Schirmung in der Nachrichtentechnik*. Springer, 1959.

[2] K. Lee and C. Baum, "Application of modal analysis to braided-shield cables," *IEEE Trans. EMC*, vol. 17, no. 3, 1975.

[3] M. Tyni, "The transfer impedance of coaxial cables with braided outer conductor," in *Proc. 3rd Int. Symp. EMC*, Wroclaw, Poland, Sept. 1976, pp. 410–418.

[4] B. Demoulin, P. Degauque, and M. Cauterman, "Shielding effectiveness of braids with high optical coverage," in *Proc. Int. Zurich. Symp. Technical Exhibition*, vol. 1, Zurich, Switzerland, Feb. 1981.

[5] F. Tesche, M. Ianoz, and T. Karlsson, *EMC analysis method and computational models*. Wiley, 1997.

[6] S. Sali, "An improved model for the transfer impedance calculations of braided coaxial cables," *IEEE Trans. EMC*, vol. 35, no. 2, pp. 139–143, May 1991.

[7] T. Kley, "Optimized single-braided cable shields," *IEEE Trans. EMC*, vol. 35, no. 1, pp. 1–9, Feb. 1993.

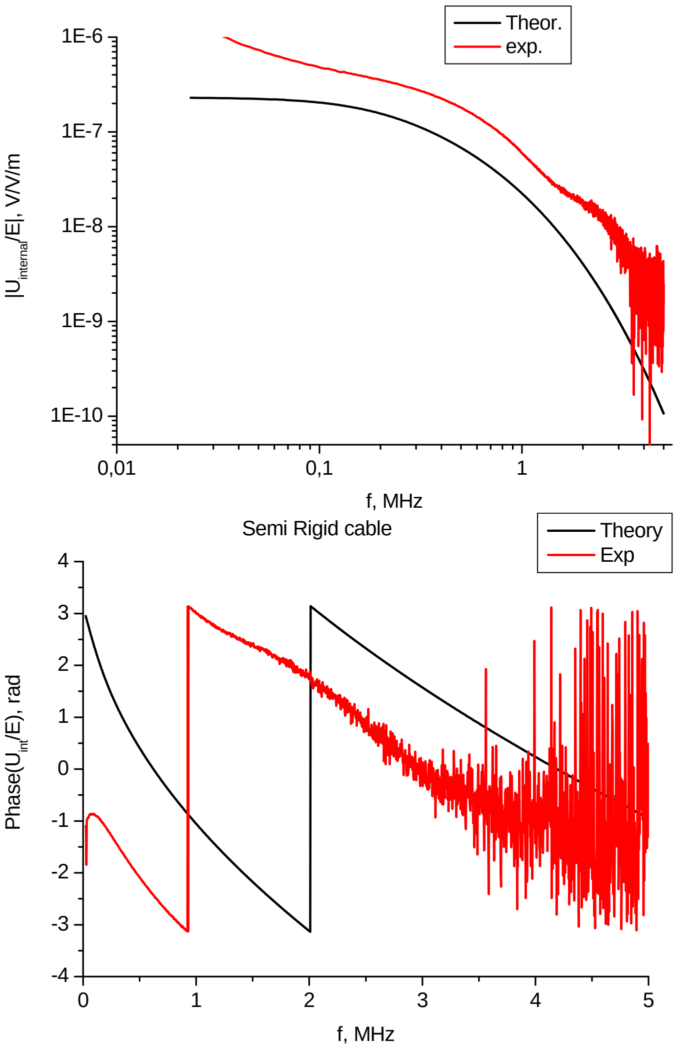

Fig. 9. Magnitude (upper graph) and phase (lower graph) of the normalized internal voltage.

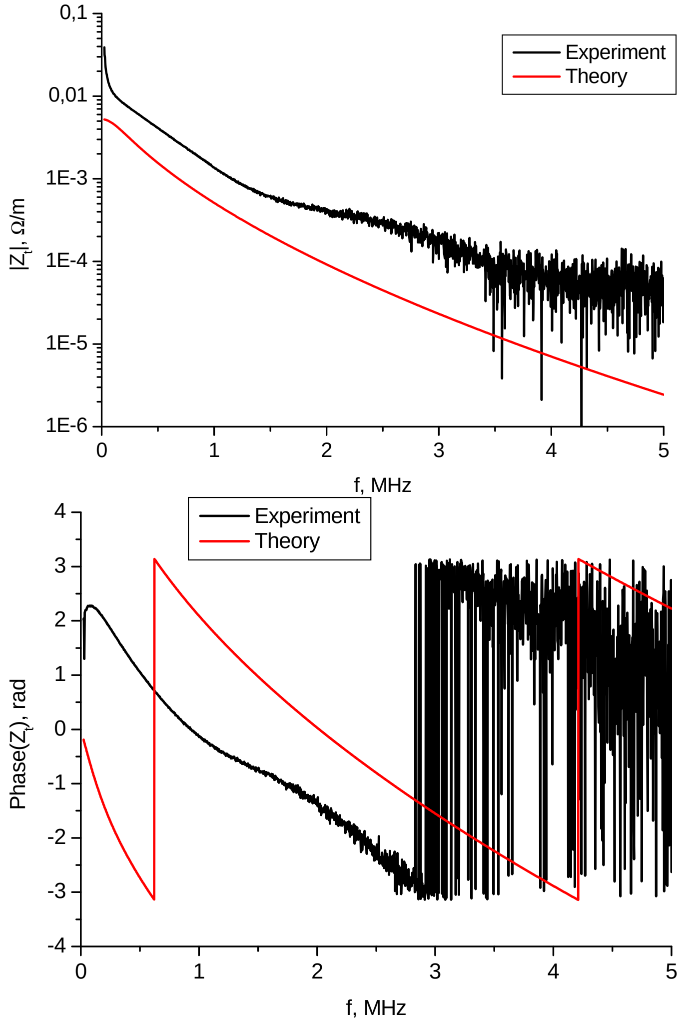

Fig. 10. Magnitude (upper graph) and phase (lower graph) of the transfer impedance of the semi rigid cable.

[8] R. Tiedemann and K.-H. Gonschorek, "Determination of the transfer impedance and the transfer admittance of coaxial cables with the current line method," in *International Symposium on EMC, Symposium Record*, Magdeburg, Germany, Oct. 1999, pp. 141–146.

[9] ——, "Messung der komplexen Kabeltransferimpedanz bis 2 GHz," in *Elektromagnetische Verträglichkeit EMV 2000*, A. Schwab, Ed. Düsseldorf, Germany: VDE Verlag, 2000, pp. 623–629.

[10] H. Haase and J. Nitsch, "High frequency model for the transfer impedance based on a generalized transmission-line theory," in *2001 IEEE EMC International Symposium, Symposium Record*, vol. 2, Aug. 2001, pp. 1242–1247.

[11] N. Korovkin, J. Nitsch, and H. Scheibe, "Improvement of cable transfer impedance measurement with the aid of the current line method," in *Proceedings of the 2003 IEEE International Symposium on Electromagnetic Compatibility*, Istanbul, Turkey, Mar. 2003.

[12] ——, "The investigation of the accuracy of the current line method," in *Proccedings of the 5th International Symposium on Electromagnetic Compatibility and Electromagnetic Ecology*, St. Petersburg, Russia, Sept. 2003, ISBN 5-7629-0542-2, (in Russian).

[13] S. Helmers and K.-H. Gonschoreck, "Determinig the coupling parameters of shielded multiconductor cables," in *14th International Symposium and Exhibition on Electromagnetic Compatibility*, Wroclaw, Poland, June 1998.

[14] S. Sali, "Cable shielding measurements at microwave frequencies," *IEEE Trans. on EMC*, vol. 46, no. 2, pp. 178–188, May 2004.

[15] L. Hoeft and J. Hofstra, "Measured electromagnetic shield performance of commonly used cables and connectors," *IEEE Trans. EMC*, vol. 30, no. 3, pp. 260–275, Aug. 1988.

[16] L. Hoeft, "A simplified relationship between surface transfer impedance and mode stirred chamber shielding effectiveness of cables and connectors," in *Int. Symp. on EMC*, Sorrento, Italy, Sept. 2002.

[17] J. Nitsch and S. Tkachenko, "Eine Transmission-Line Beschreibung für eine vertikale Halbschleife auf leitender Ebene (A transmission-line description for a vertical half-loop on a conducting plane)," in *EMV 2004*, Düsseldorf, Feb. 2004.

[18] ——, "The circular loop above conducting ground – a transmission line description," in *Electromagnetics in Advanced Applications (ICEAA 03)*, Torino, Italy, Sept. 2003, pp. 401–404.

[19] L. Weinstein, *Open resonators and open waveguides*, ser. Golem series in electromagnetics. Boulder, Colorado: Golem Press, 1969, vol. 2.

[20] T. Wu, "Theory of the thin circular loop antenna," *Journal of Mathematical Physics*, vol. 3, no. 2, pp. 1301–1304, 1962.

[21] C. Baum and H. Chang, "Fields at the center of a full circular torus and a vertically oriented torus on a perfectly conducting earth," Dec. 1972, Sensor and Simulation Notes, Note 160, http://www-e.uni-magdeburg.de/notes.

[22] C. Baum, H. Chang, and J. Martinez, "Analytical approximations and numerical techniques for the integral of the anger-weber function," Aug. 1972, Mathematical Notes, Note 25, http://www-e.uni-magdeburg.de/notes.

[23] E. Vance, *Coupling to Shielded Cables*. New York: Wiley, 1978.

[24] R. King, "The cylindrical dipole as a sensor or probe," *IEEE Trans. EMC*, vol. 24, pp. 364–367, 1982.